International Journal of
INTELLIGENT SYSTEMS AND APPLICATIONS IN ENGINEERING
ISSN:2147-6799 www.ijisae.org Original Research Paper

Multi-modal Feature Fusion with Machine Learning Approach for Leukemia Detection and Classification

I. Vinurajan[1], Dr. K. P. Sanal Kumar[2], Dr. S. Anu H. Nair[3]

Submitted: 03/02/2024 **Revised**: 11/03/2024 **Accepted**: 17/03/2024

Abstract: Leukemia is a significant cause of death worldwide and is a fatality group of cancer-related disorder that affects all age groups, mainly children and grownups. Mostly, it is related to White Blood Cells (WBC), which is supplemented by an increase in the diverse range of immature lymphocytes and affect negatively the bone marrow or bloodstream. As a result, a reliable and rapid cancer analysis is a fundamental prerequisite for effective treatment to increase the survival rate. At present, a manual diagnosis of blood samples attained by microscopic imageries is done to detect diseases that are time-consuming, less accurate, and often very slow. Moreover, the shape and appearance of leukemic cells look like ordinary cells which make detection challenging, in microscopic analysis. Currently, machine learning (ML) methods have become a better method for medical image analysis. This study presents a Multi-modal Feature Fusion with Machine Learning for Leukemia Detection and Classification (MMFFML-LDC) technique. The MMFFML-LDC technique mostly proposes to identify and categorize the occurrence of leukemia on microscopic blood images. In the MMFFML-LDC system, an initial phase of pre-processing is involved in two levels: median filtering (MF) based noise removal and adaptive histogram equalization (AHE) based contrast enhancement. Furthermore, watershed segmentation is employed to segment the pre-processed images. For feature extraction, a fusion of four ML feature extractors namely histogram of gradients (HOG), local binary pattern (LBP), scale-invariant feature transform (SIFT), and gray level co-occurrence matrix (GLCM). Finally, the detection of leukemia can be performed by the usage of a support vector machine (SVM). The performance analysis of the MMFFML-LDC technique can be studied using a blood image dataset from Kaggle. The experimental values are definite that the MMFFML-LDC system obtains better performance over other ML classifiers.

Keywords: *Feature Fusion; Leukemia Detection; Support Vector Machine; Machine Learning; Contrast Enhancement*

1. Introduction

When compared to other kinds of blood cancers, leukemia is the most general kind of tumor in dissimilar age groups, particularly for children [1]. This irregular occurrence was affected by the extreme explosion and early development of blood cells, which will harm bone marrow, the defense system, and red blood cells. In the US, above 3.5% of novel cancer people are caused by leukemia, and in the year 2018, this country stated more than 60,000 novel cases affected by this type of cancer [2]. Malignant lymphoblast or white blood cells in the blood grasp other organs like the spleen, brain, kidneys, and liver and spread to significant body tissues. Generally, there are dissimilar kinds of leukemia that hematologists in laboratories of cell transplant can distinguish/analyze depending on microscopic imageries [3]. If the image is properly spotted, a few kinds of leukemia are effortlessly recognized and differentiated when equated to others, but more equipment is needed to define basic leukemia [4]. An initial analysis of leukemia has constantly been a high task for doctors, hematologists, and researchers. Development of lymph nodes, fever, loss of weight, and pallor are the signs of leukemia [5]. Leukemia analysis is very challenging in its early phases owing to the slight nature of signs. The most general diagnosis of leukemia model is the microscopic assessment of PBS, but the gold standard only contains enchanting and analyzing samples of bone marrow [6].

Numerous research works have utilized computer-aided diagnostic (CAD) and machine learning (ML) models for laboratory analysis of images in the past two years to overwhelm the limitations of a late leukemia analysis and define its sub-groups [7]. In this research paper, blood smear imageries were assessed for discriminating, analyzing, and totaling cells in different kinds of leukemia [8]. Traditional models could not able to assess or discover shapes in a huge quantity of data. It has been established that ML is perfectly modified to deal with huge quantities of compound data and could demonstrate to be an effective tool in combating and understanding disorder [9]. Usually, expert doctors evaluate analytic tests and data of patients dependent upon the years of medicinal study and training. However, in many tasks, with prediction estimation, initial analysis, forecast of treatment issues, and decline tracking in hematologic malignancies, ML techniques have currently been established to be on par with experts [10].

[1]*Research Scholar, Department of Computer and Information Sciences, Annamalai University, Chidambaram, India.*
[2]*Assistant Professor, PG Department of Computer Science, R.V Government Arts College, Chengalpattu, India.*
[3]*Assistant Professor, Department of CSE, Annamalai University, Chidambaram, India [Deputed to WPT, Chennai].*

This study presents a Multi-modal Feature Fusion with Machine Learning for Leukemia Detection and Classification (MMFFML-LDC) technique. The MMFFML-LDC system generally intends to identify and categorize the occurrence of leukemia on microscopic blood images. In the MMFFML-LDC system, an initial phase of pre-processing was involved in two levels: median filtering (MF) based noise removal and adaptive histogram equalization (AHE) based contrast enhancement. Furthermore, watershed segmentation is employed to segment the pre-processed imageries. For feature extraction, a fusion of four ML feature extractors namely histogram of gradients (HOG), local binary pattern (LBP), scale-invariant feature transform (SIFT), and gray level co-occurrence matrix (GLCM). Finally, the detection of leukemia can be performed by the usage of a support vector machine (SVM). The performance analysis of the MMFFML-LDC technique can be studied using a blood image dataset from Kaggle.

2. Related Works

In [11], a deep feature selection (FS)-based model ResRandSVM has been projected. The projected method utilizes 7 DL techniques namely VGG16, ResNet50 ResNet152, MobileNetV2, DenseNet121, Inception V3, and EfficientNetB0 for deep feature extraction. Then, 3 FS models are utilized to remove effective and significant features. The nominated feature map is served to 4 dissimilar classifiers, Adaboost, SVM, ANN, and NB methods to categorize the imageries into normal images and leukemia. In [12], a computer-aided ALL recognition system utilizing a WOA-SVM was projected. The dimensional feature attained by uniting the developed and present features was employed to identify the feature set. The developed features were 2D-Discrete Orthonormal S-Transform with biased PCA, the quantity of revolution invariant LBP with an identical pattern, and the mean strength of Cyan of the CMYK color method. Sallam et al. [13] aim of this research is to apply an ML classification algorithm in the recognition of Acute Lymphoblastic Leukemia as malignant or benign after utilizing the GWO system in FS. The technique is based on GWO and was advanced for feature decrease.

Elrefaie et al. [14] used an enhanced criterion. After pre-processing, the K-means clustering model was applied to efficiently fragment the related nuclei from the contextual. Besides, the most noticeable features were removed utilizing an EMD depending upon the Hilbert-Huang transform. MATLAB functions are applied and equated with EMD. Ahmad et al. [15] projected an enhanced pipeline for sub-type identification of WBC that trusts TL for FE utilizing the DNN technique, monitored by a wrapper FS system based on a modified quantum-inspired evolutionary algorithm (QIEA) system. The decreased feature vector gained from QIEA was categorized with a manifold baseline classifier.

In [16], a novel hybrid model that identifies AML in blood smears is offered. The suggested model utilizes a texture-based model statistical-based method GLCM and LBP to remove the features from WBC cells. The finest features are nominated by utilizing a PSO system and their accurateness is evaluated utilizing ELM and nearest neighbor (NN)-classifier. Batool, A., and Byun [17] intend a lightweight DL-aided robust method depending upon the EfficientNet-B3 technique utilizing depth-wise separable convolution for categorizing critical lymphoblastic normal and leukemia cells in the white blood cell imageries database.

3. The Proposed Method

In this paper, we have projected a new MMFFML-LDC technique. The MMFFML-LDC technique mainly proposes to identify and categorize the occurrence of leukemia on microscopic blood imageries. Fig. 1 demonstrates the workflow of the MMFFML-LDC technique.

3.1. Preprocessing

An initial stage of pre-processing is involved in two levels: MF-based noise removal and AHE-based contrast enhancement. MF is a popular order-statistic filter due to its positive result for certain types of noise like random, Gaussian, and salt and pepper noises [18]. The noise pixel is dissimilar from the median. AHE is a sophisticated image processing method developed for improving the visual quality and enhancing the contrast of images, especially in scenarios where the classical approaches might not be sufficient. AHE locally operates, which adjusts the contrast of smaller regions based on the local histogram features, different from classical AHE, which exploits continuous transformations to the whole images. AHE effectively mitigates the over-amplification of noise and preserves local details by dividing the images into small sub-regions and independently carrying out histogram equalization, which leads to steadier enhancement through the image. This technique is especially helpful in medical imaging applications, including MRIs or X-rays, where subtle abnormalities or structures might be obscured by poor contrast. AHE allows clinicians and radiologists to extract relevant data from the images by tailoring the improvement method to certain features of all the regions, which results in better-informed treatment decisions and better diagnostic accuracy.

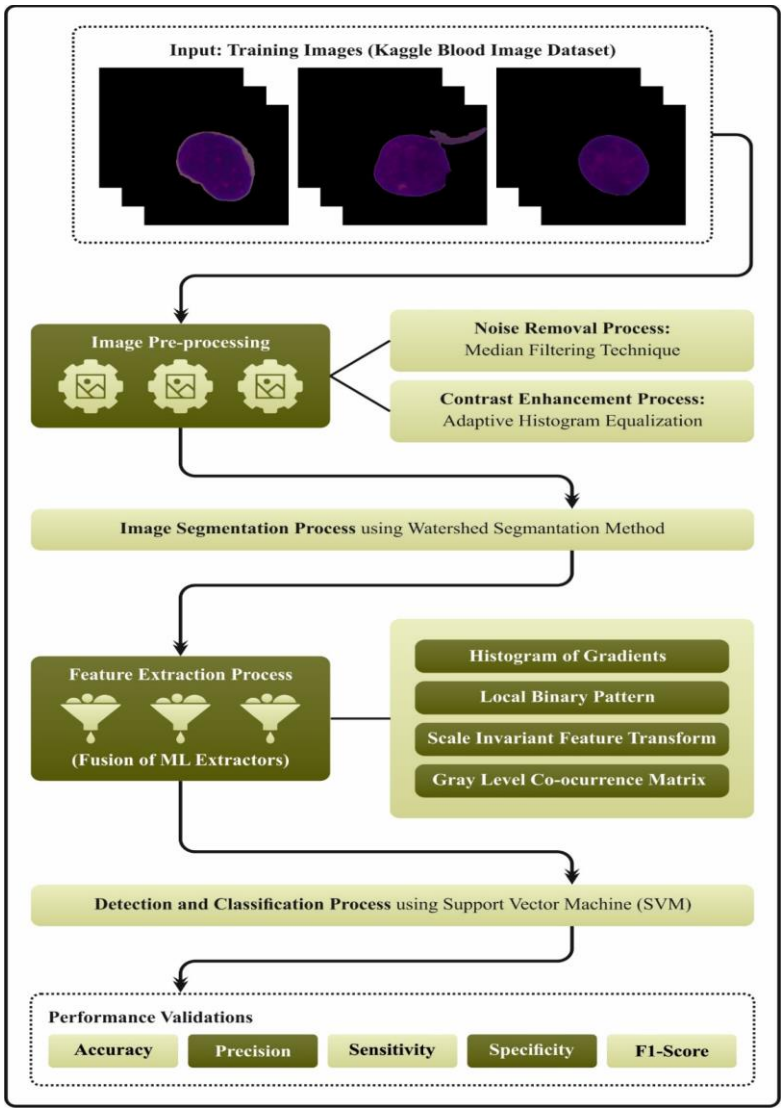

Fig. 1. Workflow of MMFFML-LDC technique

3.2. Watershed Segmentation

In this work, the watershed segmentation is used to segment the pre-processed images. Watershed segmentation is a region-based method, which uses image morphology [19]. It needs a minimum selection of one marker interior to all the objects of the image. When the object is marked, they are grown by the morphological watershed transformation. In some of the valleys, the surface is punctured and slowly immersed into the water bath. The water pours in all the punctures and starts to fill the valley. However the water from dissimilar lesions is not allowable to mix, and consequently, the dam should be constructed at the point of initial contact. This dam is the boundary of the water basin as well as the image object. The image is considered a topographical landscape with valleys and ridges in watershed segmentation. The elevation value is commonly determined by the gray value of the gradient magnitude or the corresponding pixel. The watershed transform is used to decompose the image into catchment basins based on the 3D representation. For local minima, a catchment basin includes every point whose track of steepest descent ends at this lowest. The watershed divides the basin from one another. The watershed transformation completely decomposes the image and thereby allocates all the pixels to a watershed or a region.

3.3. Feature Fusion Process

For feature extraction, a fusion of four ML feature extractors namely HOG, LBP, SIFT, and GLCM.

3.3.1. HOG Method

Local object shape and appearance are considered the edge detection or distribution of local intensity gradients [20]. HOG feature is evaluated by enchanting an orientation histogram of edge intensity in the local area. The authors stated that better outcomes are attained by the SIFT descriptor. HOG feature is extracted from 16×16 local regions. Initially, gradient magnitude and orientations are evaluated at all the pixels. The Sobel filter is used for obtaining the gradient magnitude and orientations. The edge gradients $m(x, y)$ and orientation $\theta(x, y)$ are evaluated by the x- and y-directional gradients

$dx(x,y)$ and $dy(x,y)$ calculated by the Sobel filter as follows:

$$m(x,y) = \sqrt{dx(x,y)^2 + dy(x,y)^2}$$

$$\theta(x,y) = \{tan^{-1}\left(\frac{dy(x,y)}{dx(x,y)}\right) - \pi \; if \; dx(x,y) < 0 \; and \; dy(x,y) < 0 \; tan^{-1}\left(\frac{dy(x,y)}{dx(x,y)}\right) + \pi \; if \; dx(x,y) < 0 \; and \; dy(x,y) > 0 \; tan^{-1}\left(\frac{dy(x,y)}{dx(x,y)}\right) \; otherwise \quad (1)$$

This local area is split into smaller spatial regions named "cells". The size of cell is 4x4 pixels. The overall amount of HOG features converts $128 = 8\text{x}(4\text{x}4)$ and they create a HOG feature vector. to provide less significance to gradients and to evade abrupt fluctuations in the descriptor with slight variations in the window position, a Gaussian weight with σ equivalent to one-half of the descriptor window assigns weight to the size of all the pixels.

The HOG feature vector is the local shape having edge data at plural cells. The HOG has a flatter distribution in flatter regions like a wall of a building or a ground. In contrast, in the edge between a background and an object, one of the components in the histogram has a larger value and it specifies the edge direction. HOG feature is vigorous to the local photometric and geometric invariants. The authors removed a series of HOG feature vectors from each location in the image grid and utilized them for identification. Here, the HOG features are removed from each location on the grid of 6×14 input images with pixels 56×120.

3.3.2. LBP Method

There are different techniques to remove the most relevant feature from the preprocessed imageries to perform [21]. The LBP method is considered one of the feature extraction techniques. Ojala et al in 1996 proposed a new approach named LBP which describes the texture and shape of the digital images. This can be performed by dividing the image into many smaller areas where the feature was extracted.

This includes binary patterns that delineate the pixels surrounding the region. The features obtained from the region are concatenated into the single feature histogram that forms image representation. Then, Images are compared by evaluating the distance (similarity) between the histograms. The LBP technique provides better outcomes according to several studies, in terms of discrimination performance and speed. Due to the shape and texture of images, the technique seems to be most vigorous against images with different lighting conditions, different facial expressions, aging of persons, and image rotation.

3.3.3. SIFT Method

SIFT is invariant to measure, brightness, and rotation transformations [22]. SIFT features are used for combining with other kinds of feature matching and computing large feature datasets. It is attained by the infrared rays that defend against spoof attacks, external damages, and impersonation. In this work, segmentation can be performed by the SIFT model. The SIFT method is applied for image recognition and matching. Using the difference of Gaussian (DOG), SIFT evaluates the scale space extrema to discover the key point localization for removing the lower contrast point. Lastly, a key point orientation task is performed according to the local image gradients. Next, we have found the image features for all the key points using image gradient orientation and magnitude. Fig. 2 depicts the architecture of SIFT. The SIFT technique is given below,

- Gaining the target image
- Calculation of image descriptor.
- Calculation of the scale space extrema of the image utilizing the DOG function
- Discover the key point of localization

The local extrema estimation of key points (x,y) is represented as

$$D(x,y,\sigma) = (G(x,y,\sigma) - G(x,y,\sigma))^* I(x,y) \quad (2)$$

$$D(x,y,\sigma) = L(x,y,s\sigma) - L(x,y,\sigma)$$

$$L(x,y,\sigma) = G(x,y,\sigma)^* I(x,y) \quad (3)$$

$$G(x,y,\sigma) = \frac{1}{2\pi\sigma^2} e^{-(x^2+y^2)/2} \quad (4)$$

Where $L(x,y,\sigma)$ characterizes Gaussian Smoothed imagery at the key points with σ and σ is a scaling parameter. The $D(x,y,\sigma)$ is employed to discover the interpolation for all key points

$$D(x) = D + \frac{\lambda D^T}{\lambda x} x + \frac{1}{2} x^T \frac{\lambda^2 D}{\lambda x^2} x \quad (5)$$

The gradient magnitude $m(x,y)$ of image and orientation $\theta(x,y)$ is calculated by.

$$m(x,y) = \sqrt{(L(x+1,y) - L(x-1,y))^2 + (L(x,y+1) - L(x,y-1))}$$

$$\theta(x,y) = tan^{-1}\left(\frac{L(x,y+1)-L(x,y-1)}{L(x+1,y)-L(x-1,y)}\right) \quad (7)$$

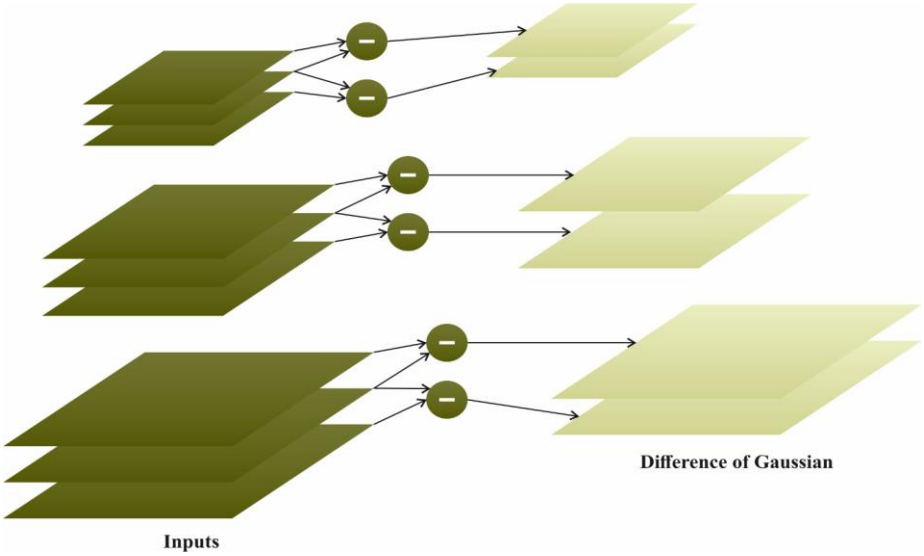

Fig. 2. Structure of SIFT

3.3.4. GLCM Method

This converts the image of the host into the matrix which reacts with a definite distance to the place of the pixel value [23]. This evaluated the mutual occurrence of dual-pixel pair values with dissimilar directions and distances which reflect vertical, horizontal, and diagonal directions.

$$G_{dist}^{theta}(i,j) = \{((x,y),(m,n()I(x,y)m,n)j\}) \quad (8)$$

where $(x,y),(m,n) \in N_x \times N_y$

$$(m,n) = (x + disr \times theta_1, y + dist \times theta_2) \quad (9)$$

Whereas G_{dist}^{theta} refers to the gray-level co-occurrence matrix of distance $dist$ and angle $theta$. $I(x,y)$ and $I(m,n)$ denote the pixel intensity at location (m,n). Values of $theta_1$ and $theta_2$ are based on the direction.

In existing plays, local binary patterns are normally named histograms for extraction, and their frequency does not contain the pattern. By utilizing GLCM in numerous lengths and directions, the Dominant Rotated Local Binary Pattern (DRLBP) feature extraction procedure is executed.

$$Img = DRLBP(dwtcoefficients)$$

$$GLCM_{dist}^{theta}(Img) = G_{dist}^{theta}(i,j) \forall (i,j) \in Img \quad (10)$$

Whereas, Img represents the *DRLBP* image map. The 4 mixtures of *GLCM* have been utilized to generate 4 dissimilar feature vectors.

$$FV_1(I)\left[GLCM_1^{0^\circ} GLCM_1^{45^\circ} GLCM_1^{90^\circ} GLCM_1^{135^\circ}\right] \quad (11)$$

$$FV_2(I)\left[GLCM_2^{0^\circ} GLCM_2^{45^\circ} GLCM_2^{90^\circ} GLCM_2^{135^\circ}\right] \quad (12)$$

$$FV_3(I)\left[GLCM_1^{0^\circ} GLCM_1^{45^\circ} GLCM_2^{0^\circ} GLCM_2^{45^\circ}\right] \quad (13)$$

$$FV_4(I)\left[GLCM_1^{0^\circ} GLCM_1^{90^\circ} GLCM_2^{0^\circ} GLCM_2^{90^\circ}\right] \quad (14)$$

More spatial data is accessible in pixels of neighboring that remove the frequency of these patterns in another direction by attaining GLCM in specific distances and directions.

3.4. Leukemia Detection using SVM

Finally, the recognition of leukemia can be performed by the usage of SVM. Cortes and Vapnik first projected SVM, which is a chosen model in this study [24]. It generally is appropriate for supervised learning and employed for regression, outlier recognition, and classification. The main intention of SVM is to examine a hyperplane in an N-dimension feature space which exactly keeps apart the distinct class points. The support vector enhances the boundary among the classifiers. Hyperplanes perform as the optimal borders that make the feature data. SVM is a novel learning technique, and the main dissimilarity between SVM and ML methods is that the SVM decreases the feasible obligation rather than dropping the error of classification. This model's function is to separate feature points utilizing the hyperplane to the numerous classes they fit. For a dual-dimension space, the central separator among the dual classes is named discriminator. Assume that the distance between every class data point and the classifier is equivalent to one.

Let x be a vector of feature whereas $x \in R^n$,

y denotes a class while $y \in \{1,-1\}$,

b and w refer to the SVM parameters acquired utilizing the training set,

$x^{(i)}, y^{(i)}$: i^{th} sample of the dataset between N sample training set,

Where, the class $y(i)$ for vector $x(i)$ was defined by:

$$y^{(i)} = \{-1\ if\ w^T x^{(i)} + b \leq -1\ 1\ if\ w^T x^{(i)} + b \geq 1 \quad (15)$$

To separate the classes of data points, numerous probable hyperplanes are potential. The foremost aim is to identify a plane that contains the highest border. Utilizing Eq. (15) the optimum margin (M) was set by:

$$M = \frac{(|b+1| - |b-1|)}{||w||} = \frac{2}{||w||}. \quad (16)$$

Also, SVM was prolonged to resolve multi-class issues utilizing the one-against-one technique. A similar model has been used to learn the damage identification task with 5 dissimilar damage classes. In this model, for n classes count, there are $n \times \frac{(n-1)}{2}$ classifications and everyone trains the data from dual classes.

4. Experimental Validation

In this paper, the performance analysis of the MMFFML-LDC technique is tested by employing a leukemia classification dataset from Kaggle [25]. The dataset contains 3875 samples with 1927 normal images and 1948 ALL classes as definite in Table 1. Fig. 3 signifies the sample of original, pre-processed, and segmented images. Fig. 4 portrays the sample images of extracted features.

Table 1 Details of dataset

Classes	**No. of Samples**
NORMAL	1927
Acute Lymphoblastic Leukemia (ALL)	1948
Total Samples	**3875**

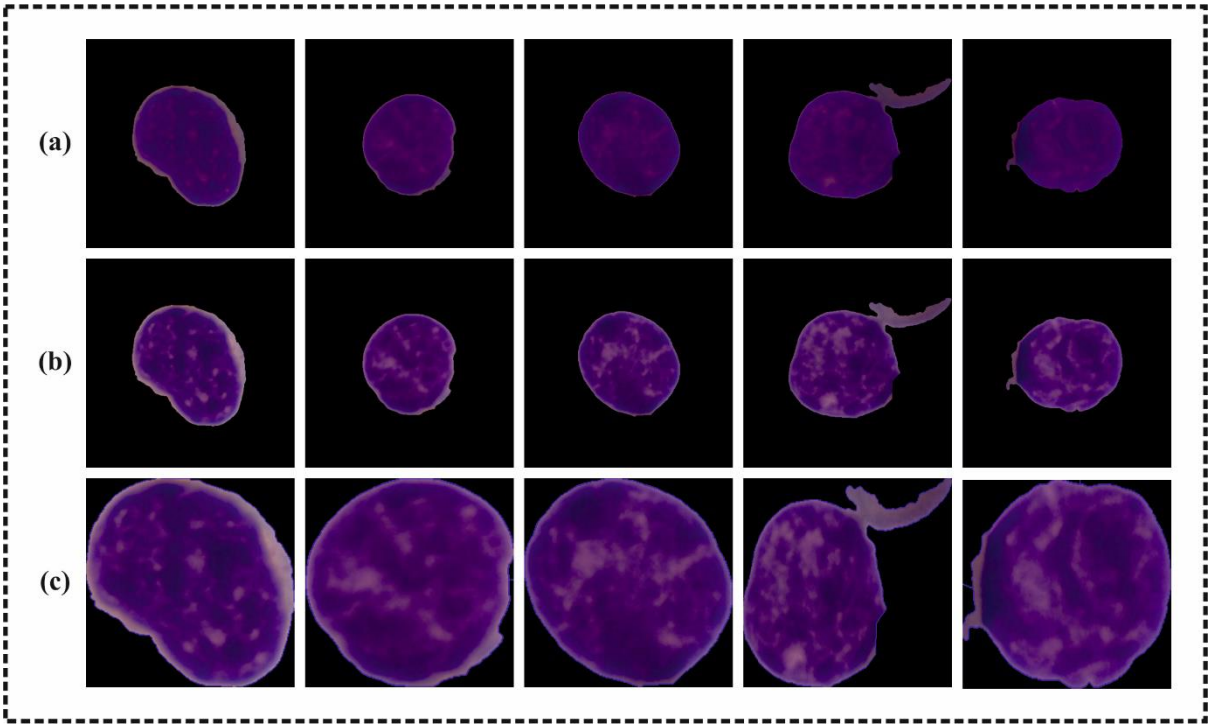

Fig. 3. a) Original Images b) Preprocessed Images c) Segmented Images

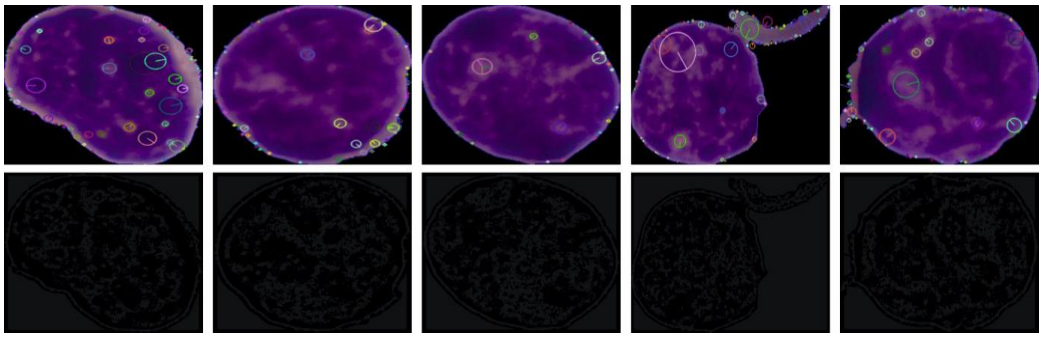

Fig. 4. Sample Images of Extracted Features

Fig. 5 institutes the classifier results of the MMFFML-LDC technique under training and testing data. Fig. 5a describes the confusion matrices presented by the MMFFML-LDC approach. The figure shows that the MMFFML-LDC methodology is well-known and categorizes all 2 classes exactly. Also, Fig. 5b exposes the PR study of the MMFFML-LDC technique. The figure defined that the MMFFML-LDC system has got greatest performance of PR under all classes. Finally, Fig. 5c establishes the ROC study of the MMFFML-LDC technique. The outcome described that the MMFFML-LDC approach has caused in proficient results with the greatest values of ROC under different classes.

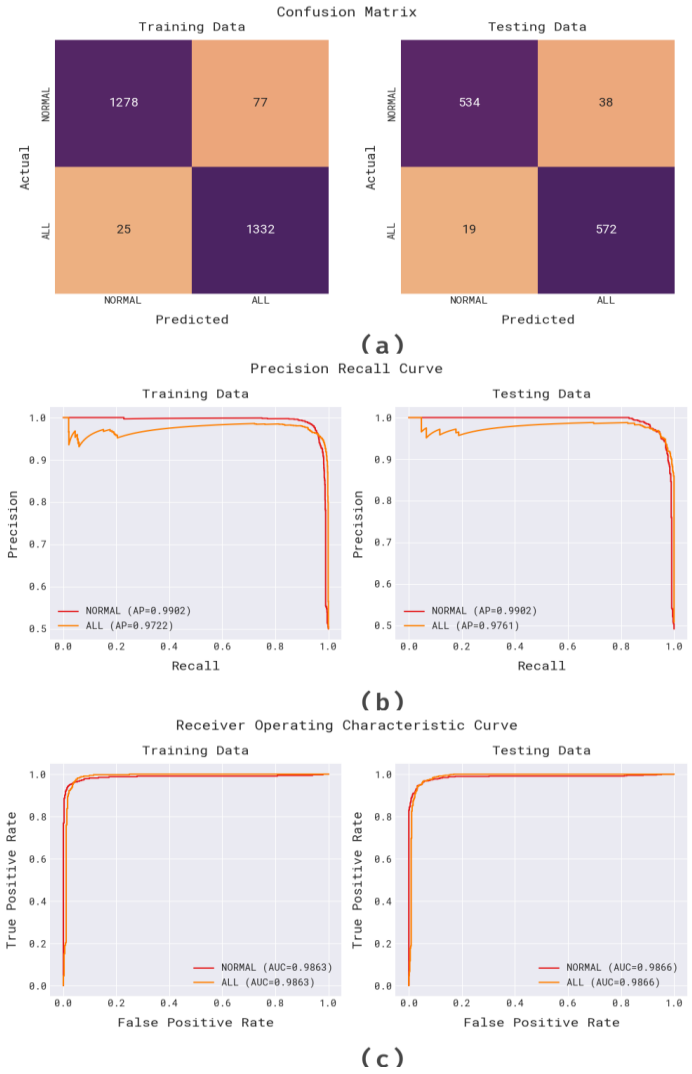

Fig. 5. Training and Testing Data a) Confusion Matrix b) PR Curve c) ROC Curve

Table 2 denotes an overall leukemia detection result of the MMFFML-LDC model under training and testing data. In Fig. 6, the complete leukemia detection outcomes of the MMFFML-LDC system are provided. The outcomes identified that the MMFFML-LDC model correctly recognized the normal and ALL classes. With normal class, the MMFFML-LDC method provides $an\ accu_y$ of 96.24%, $prec_n$ of 98.08%, $sens_y$ of 94.32%, $spec_y$ of

98.16%, and $F1_{score}$ of 96.16%. Likewise, with ALL classes, the MMFFML-LDC approach delivers an $accu_y$ of 96.24%, $prec_n$ of 94.54%, $sens_y$ of 98.16%, $spec_y$ of 94.32%, and $F1_{score}$ of 96.31%.

Table 2 Leukemia detection of MMFFML-LDC technique under training and testing data

Data Split	Measures	NORMAL	ALL	Overall
Training	**Accuracy**	96.24	96.24	96.24
	Precision	98.08	94.54	96.31
	Sensitivity	94.32	98.16	96.24
	Specificity	98.16	94.32	96.24
	F1-Score	96.16	96.31	96.24
Testing	**Accuracy**	95.10	95.10	95.10
	Precision	96.56	93.77	95.17
	Sensitivity	93.36	96.79	95.07
	Specificity	96.79	93.36	95.07
	F1-Score	94.93	95.25	95.09

In Fig. 7, the detailed leukemia recognition results of the MMFFML-LDC approach are provided. The outcomes identified that the MMFFML-LDC system correctly recognized the normal and ALL classes. With normal class, the MMFFML-LDC technique provides $an\ accu_y$ of 95.10%, $prec_n$ of 96.56%, $sens_y$ of 93.36%, $spec_y$ of 96.79%, and $F1_{score}$ of 94.93%. Also, with ALL classes, the MMFFML-LDC model provides an $accu_y$ of 95.10%, $prec_n$ of 95.17%, $sens_y$ of 95.07%, $spec_y$ of 95.07%, and $F1_{score}$ of 95.09%.

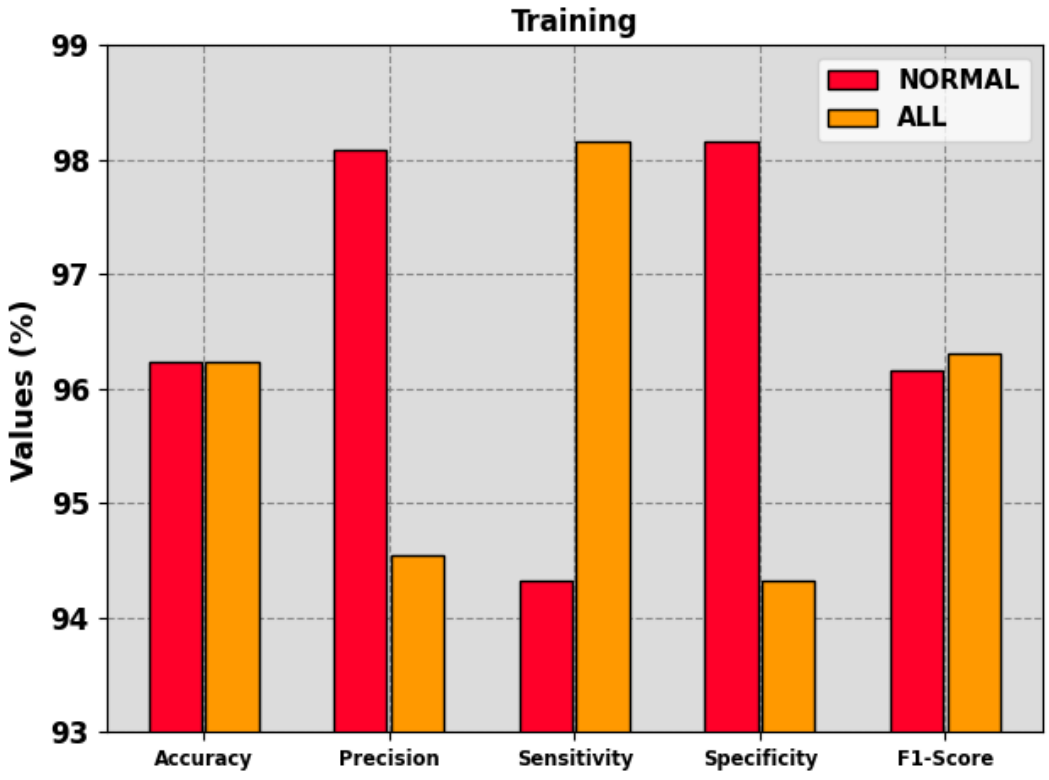

Fig. 6. Leukemia detection of MMFFML-LDC technique under training data

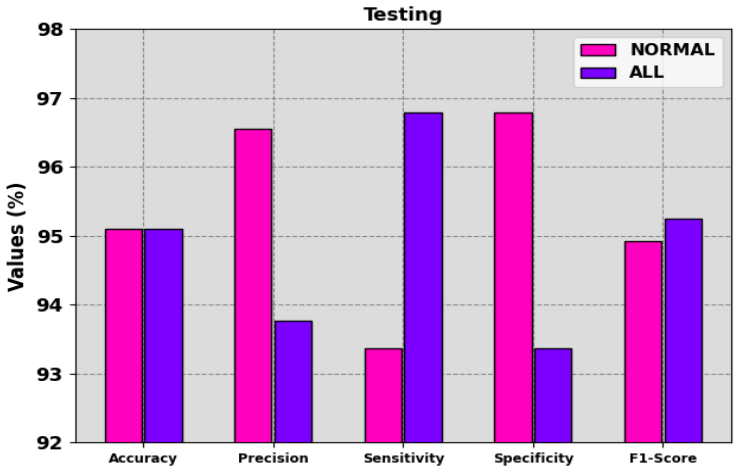

Fig. 7. Leukemia detection of MMFFML-LDC technique under testing data

In Table 3, a brief comparison study of the MMFFML-LDC model with current DL techniques is set [9, 17]. In Fig. 8, the comparative results of the MMFFML-LDC technique in terms of $sens_y$ and $spec_y$ are given. The results highlighted that the MMFFML-LDC approach gains better performance. Based on $sens_y$, the MMFFML-LDC model displays a greater $sens_y$ of 96.24% while the CNN, VT, CNN-ECA, GAO, and SVM-cell energy feature systems portray a lower $sens_y$ of 92.43%, 92.44%, 91.74%, 91.82%, and 91.32%, correspondingly. Moreover, based on $spec_y$, the MMFFML-LDC approach exhibits a greater $spec_y$ of 96.24% whereas the CNN, VT, CNN-ECA, GAO, and SVM-cell energy feature models portray lesser $spec_y$ of 89.18%, 93.24%, 89.56%, 91.67%, and 88.99%, respectively.

Table 3 Comparative analysis of MMFFML-LDC system with recent DL models

Methods	$Accu_y$	$Prec_n$	$Sens_y$	$Spec_y$	$F1_{Score}$
CNN Model	88.25	88.72	92.43	89.18	91.77
Vision Transformer	88.20	91.70	92.44	93.24	87.76
CNN-ECA Module	91.10	90.85	91.74	89.56	92.49
GAO-Based Method	93.84	89.01	91.82	91.67	88.22
SVM-Cell Energy Feature	94.00	92.20	91.32	88.99	93.88
MMFFML-LDC	96.24	96.31	96.24	96.24	96.24

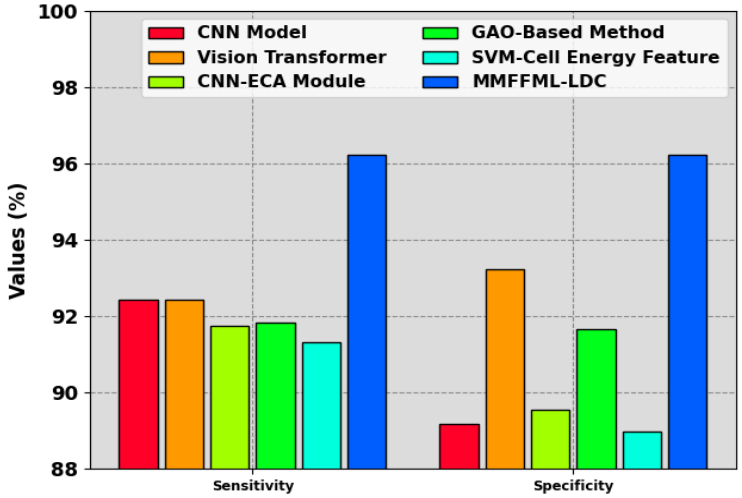

Fig. 8. $Sens_y$ and $spec_y$ analysis of MMFFML-LDC technique with recent DL models

In Fig. 9, the comparative outcomes of the MMFFML-LDC system in terms of $accu_y$, $prec_n$, and $F1_{score}$ are given. The results emphasized that the MMFFML-LDC approach gets better performance. Based on $accu_y$, the MMFFML-LDC model exhibits a greater $accu_y$ of 96.24% while the CNN, VT, CNN-ECA, GAO, and SVM-cell energy feature models portray lower $accu_y$ of 88.25%, 88.20%, 91.10%, 93.84%, and 94.00%, correspondingly. Additionally, based on $prec_n$, the MMFFML-LDC method reveals a greater $prec_n$ of 96.31% whereas the CNN, VT, CNN-ECA, GAO, and SVM-cell energy feature models represent lesser $prec_n$ of 88.72%, 91.70%, 90.85%, 89.01%, and 92.20%, correspondingly. Lastly, based on $F1_{score}$, the MMFFML-LDC approach exhibits a higher $F1_{score}$ of 96.24% whereas the CNN, VT, CNN-ECA, GAO, and SVM-cell energy feature models portray a lower $F1_{score}$ of 91.77%, 87.76%, 92.49%, 88.22%, and 93.88%, correspondingly.

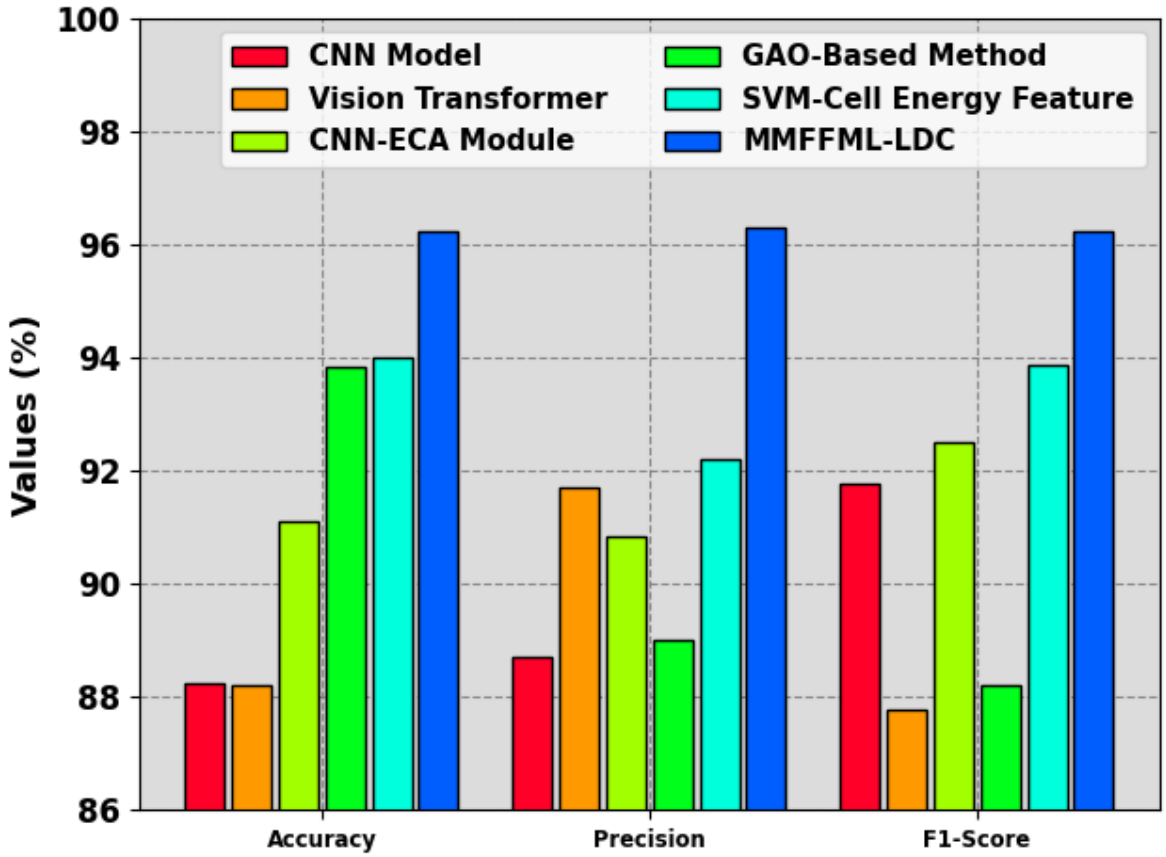

Fig. 9. Comparative analysis of MMFFML-LDC technique with recent DL models

Thus, the MMFFML-LDC technique can be applied for an effectual leukemia detection process.

5. Conclusion

In this paper, we have developed an innovative MMFFML-LDC approach. The MMFFML-LDC technique generally proposes to identify and categorize the occurrence of leukemia on microscopic blood images. In the MMFFML-LDC system, an initial phase of pre-processing is involved in two levels: MF-based noise removal and AHE-based contrast enhancement. Furthermore, watershed segmentation is employed to segment the pre-processed imageries. For feature extraction, a fusion of four ML feature extractors namely HOG, LBP, SIFT, and GLCM. Finally, the detection of leukemia can be executed by the usage of SVM. The performance analysis of the MMFFML-LDC system can be studied using a blood image dataset from Kaggle. The experimentation values indicated that the MMFFML-LDC system obtains better performance over other ML classifiers.

References

[1] Ramagiri, A., Jahnavi, V., Gottipati, S., Monica, C., Afrin, S., Jyothi, B. and Chinnaiyan, R., 2023, March. Image Classification for Optimized Prediction of Leukemia Cancer Cells using Machine Learning and Deep Learning Techniques. In *2023 International Conference on Innovative Data Communication Technologies and Application (ICIDCA)* (pp. 193-197). IEEE.

[2] Arivuselvam, B. and Sudha, S., 2022. Leukemia classification using the deep learning method of

CNN. *Journal of X-ray science and technology*, *30*(3), pp.567-585.

[3] Abhishek, A., Jha, R.K., Sinha, R. and Jha, K., 2023. Automated detection and classification of leukemia on a subject-independent test dataset using deep transfer learning supported by Grad-CAM visualization. *Biomedical Signal Processing and Control*, *83*, p.104722.

[4] Abhishek, A., Jha, R.K., Sinha, R. and Jha, K., 2022. Automated classification of acute leukemia on a heterogeneous dataset using machine learning and deep learning techniques. *Biomedical Signal Processing and Control*, *72*, p.103341.

[5] Gondal, C.H.A., Irfan, M., Shafique, S., Bashir, M.S., Ahmed, M., Alshehri, O.M., Almasoudi, H.H., Alqhtani, S.M., Jalal, M.M., Altayar, M.A. and Alsharif, K.F., 2023. Automated Leukemia Screening and Sub-types Classification Using Deep Learning. *Computer Systems Science & Engineering*, *46*(3).

[6] Hagar, M., Elsheref, F.K. and Kamal, S.R., 2023. A New Model for Blood Cancer Classification Based on Deep Learning Techniques. *International Journal of Advanced Computer Science and Applications*, *14*(6).

[7] Mallick, P.K., Mohapatra, S.K., Chae, G.S. and Mohanty, M.N., 2023. Convergent learning–based model for leukemia classification from gene expression. *Personal and Ubiquitous Computing*, *27*(3), pp.1103-1110.

[8] Das, P.K. and Meher, S., 2021. An efficient deep convolutional neural network based detection and classification of acute lymphoblastic leukemia. *Expert Systems with Applications*, *183*, p.115311.

[9] Bukhari, M., Yasmin, S., Sammad, S., El-Latif, A. and Ahmed, A., 2022. A deep learning framework for leukemia cancer detection in microscopic blood samples using squeeze and excitation learning. *Mathematical Problems in Engineering*, *2022*.

[10] Arivuselvam, B. and Sudha, S., 2022. Leukemia classification using the deep learning method of CNN. *Journal of X-ray science and technology*, *30*(3), pp.567-585.

[11] Sulaiman, A., Kaur, S., Gupta, S., Alshahrani, H., Reshan, M.S.A., Alyami, S. and Shaikh, A., 2023. ResRandSVM: Hybrid Approach for Acute Lymphocytic Leukemia Classification in Blood Smear Images. *Diagnostics*, *13*(12), p.2121.

[12] Saikia, R., Sarma, A. and Shuleenda Devi, S., 2024. Optimized Support Vector Machine Using Whale Optimization Algorithm for Acute Lymphoblastic Leukemia Detection from Microscopic Blood Smear Images. *SN Computer Science*, *5*(5), p.439.

[13] Sallam, N.M., Saleh, A.I., Arafat Ali, H. and Abdelsalam, M.M., 2022. An efficient strategy for blood diseases detection based on grey wolf optimization as feature selection and machine learning techniques. *Applied Sciences*, *12*(21), p.10760.

[14] Elrefaie, R.M., Mohamed, M.A., Marzouk, E.A. and Ata, M.M., 2024. A robust classification of acute lymphocytic leukemia-based microscopic images with supervised Hilbert-Huang transform. *Microscopy Research and Technique*, *87*(2), pp.191-204.

[15] Ahmad, R., Awais, M., Kausar, N., Tariq, U., Cha, J.H. and Balili, J., 2023. Leukocytes classification for leukemia detection using quantum inspired deep feature selection. *Cancers*, *15*(9), p.2507.

[16] Mohan, A., Beshir, K. and Kebede, A., 2024. Acute myelogenous leukaemia detection in blood microscope images using particle swarm optimisation. *International Journal of Computational Vision and Robotics*, *14*(3), pp.250-263.

[17] Batool, A. and Byun, Y.C., 2023. Lightweight EfficientNetB3 model based on depthwise separable convolutions for enhancing classification of leukemia white blood cell images. *IEEE Access*.

[18] Dinç, İ., Dinç, S., Sigdel, M., Sigdel, M.S., Aygün, R.S. and Pusey, M.L., 2015. DT-Binarize: A decision tree based binarization for protein crystal images. In Emerging trends in image processing, computer vision and pattern recognition (pp. 183-199). Morgan Kaufmann.

[19] Jamil, M.M.A., Oussama, L., Hafizah, W.M., Abd Wahab, M.H. and Johan, M.F., 2019. Computational automated system for red blood cell detection and segmentation. In *Intelligent Data Analysis for Biomedical Applications* (pp. 173-189). Academic Press.

[20] Kobayashi, T., Hidaka, A. and Kurita, T., 2008. Selection of histograms of oriented gradients features for pedestrian detection. In *Neural Information Processing: 14th International Conference, ICONIP 2007, Kitakyushu, Japan, November 13-16, 2007, Revised Selected Papers,*

Part II 14 (pp. 598-607). Springer Berlin Heidelberg.

[21] Rahim, M.A., Hossain, M.N., Wahid, T. and Azam, M.S., 2013. Face recognition using local binary patterns (LBP). *Global Journal of Computer Science and Technology*, *13*(4), pp.1-8.

[22] Kasiselvanathan, M., Sangeetha, V. and Kalaiselvi, A., 2020. Palm pattern recognition using scale invariant feature transform. *International Journal of Intelligence and Sustainable Computing*, *1*(1), pp.44-52.

[23] Garg, M., Malhotra, M. and Singh, H., 2021. A novel machine-learning framework-based on LBP and GLCM approaches for CBIR system. *Int. Arab J. Inf. Technol.*, *18*(3), pp.297-305.

[24] Harirchian, E., Lahmer, T., Kumari, V. and Jadhav, K., 2020. Application of support vector machine modeling for the rapid seismic hazard safety evaluation of existing buildings. *Energies*, *13*(13), p.3340.

[25] https://www.kaggle.com/datasets/andrewmvd/leukemia-classification